Geophysical Research Letters

RESEARCH LETTER
10.1029/2021GL092558

Key Points:

- Analysis of model large ensembles shows stronger cooling in the Arctic than in the Antarctic in response to symmetric volcanic forcing
- Arctic sea ice area and volume increase for several years after the eruption while Antarctic sea ice area and volume show little response
- The damped Southern Ocean cooling is analogous to the weak warming in the short-term response to greenhouse gas forcing in that region

Supporting Information:

Supporting Information may be found in the online version of this article.

Correspondence to:

A. G. Pauling,
apauling@uw.edu

Citation:

Pauling, A. G., Bushuk, M., & Bitz, C. M. (2021). Robust inter-hemispheric asymmetry in the response to symmetric volcanic forcing in model large ensembles. *Geophysical Research Letters*, *48*, e2021GL092558. https://doi.org/10.1029/2021GL092558

Received 25 JAN 2021
Accepted 12 APR 2021

Robust Inter-Hemispheric Asymmetry in the Response to Symmetric Volcanic Forcing in Model Large Ensembles

Andrew G. Pauling[1], Mitchell Bushuk[2], and Cecilia M. Bitz[1]

[1]Department of Atmospheric Sciences, University of Washington, Seattle, WA, USA, [2]Geophysical Fluid Dynamics Laboratory, NOAA, Washington DC, NJ, USA

Abstract The climate response to volcanic eruptions in the twentieth century is difficult to separate from the influence of anthropogenic greenhouse gas forcing and internal variability. Here, we make use of recently available large ensembles of Earth-system model simulations to better understand the forced climate response to contemporary volcanic eruptions. While the Pinatubo eruption in June 1991 resulted in approximately symmetric forcing between the Northern and Southern Hemispheres, the ensemble-mean simulated temperature and sea ice responses it produces are asymmetric. The strongest cooling and sea ice expansion occur in the Arctic, while the responses in the Antarctic are weak. The damped high-latitude Southern Hemisphere response to volcanic forcing is analogous to the fast response to increased greenhouse gas concentrations, despite the differing physical nature of the forcing. We find that Arctic cooling in response to a Pinatubo-scale eruption may not occur due to the high internal variability in that region

Plain Language Summary Volcanic eruptions can have a large short-term influence on global climate due to the injection of reflective particles into the stratosphere that cool the planet. However, the impact of twentieth century volcanic eruptions on climate has been difficult to distinguish from the impact of other factors such as anthropogenic greenhouse gas forcing and natural variability. Averaging the response over many climate model simulations, each with different natural variations but the same climate, suppresses the influence of natural variability and allows the true response to become more evident. The eruption of Pinatubo in June 1991 spread reflective particles into the stratosphere roughly evenly between the Northern and Southern Hemispheres. However, the changes in temperature and sea ice it produced were quite different between the two hemispheres. The area of Arctic sea ice grew, and the region cooled after the eruption, while the Antarctic showed little response. Previously, this result had only been shown in single climate models with idealized conditions where all forcing except the volcanoes was held fixed. Our results show that this response is a robust feature of the climate response to volcanic eruptions, and is not strongly dependent on the particular climate model used.

1. Introduction

Volcanic eruptions, particularly those that occur in the tropics, can have a large impact on climate (e.g., Robock, 2000) when sulfate aerosols reach the stratosphere. The climate impact is "globalized" through dispersal of the stratospheric aerosols zonally by the climatological zonal winds and to higher latitudes by the Brewer-Dobson circulation (Robock, 2000). Yet, studies show that the spatial pattern of the climate response to volcanic eruptions is uneven and depends strongly on the latitudinal distribution of the stratospheric sulfate loading (e.g., Toohey et al., 2019; Yang et al., 2019; Zanchettin et al., 2014). The three major volcanic eruption of the last century: Agung in March 1963, El Chichon in April 1982, and Pinatubo in June 1991, produced aerosol distributions that were Southern Hemisphere focused, Northern Hemisphere focused, and approximately symmetric, respectively. Thus, one might expect that these three different scenarios would produce high-latitude climate responses concentrated in the hemisphere in which the forcing is predominantly located.

Low-latitude volcanic eruptions affect sea ice when the stratospheric volcanic aerosols are transported to high latitudes (e.g., Ding et al., 2014; Gagne et al., 2017; Stenchikov et al., 2009; Zanchettin et al., 2014). The study of Zanchettin et al. (2014) showed that the sea ice response to hemispherically symmetric volcanic forcing alone in a climate model is hemispherically asymmetric. They found that Arctic sea ice extent

increased in response to a Pinatubo-sized eruption, while Antarctic sea ice responded only to very large "super-volcano" eruptions. This asymmetry was attributed to the differing changes in meridional heat transport in each hemisphere, as well as local feedbacks in the Antarctic region.

The study of Yang et al. (2019) showed that the zonal-mean temperature response in simulations forced only with volcanic forcing that is approximately symmetric between the two hemispheres (like Pinatubo) is strongly asymmetric, with much greater cooling in the Arctic than in the Southern Ocean and Antarctic regions. However, this asymmetry is not discussed further in their paper, and it is not clear whether this response is a robust feature of the climate system, or a model-dependent response to volcanic forcing.

These previous studies have conducted model experiments with single-model ensembles only. The recent compilation of large ensembles of historical simulations conducted with models that participated in the Coupled Model Intercomparison Project Phase 5 (CMIP5; Deser et al., 2020), and the recent efforts of many modeling centers to run large ensembles with historical forcing with their models participating in the Coupled Model Intercomparison Project Phase 6 (CMIP6, Eyring et al., 2016) allows a unique opportunity to assess the robustness of the forced response of polar regions to volcanic eruptions across many models and realizations. By greatly reducing the internal variability, the ensemble means allow us the opportunity to assess whether the response to volcanoes is robust in the presence of other historical climate forcings.

In this paper, we make use of these recently available large ensembles of historical simulations from CMIP5- and CMIP6-generation Earth system models to evaluate the high-latitude climate response during large volcanic eruptions. In contrast to previous work we investigate the impact of volcanic eruptions in the presence of other historical climate forcing, since that is what occurred in nature. The use of these large ensembles allows us to average climate variables over relatively short periods of time while still reducing the influence of natural variability. Thus, while other forcings such as anthropogenic greenhouse gases and aerosols are present in these simulations, the impact of the volcanic eruptions dominates over the signal from other forcings over short timescales and allows us to increase the signal-to-noise ratio of the climate response.

2. Data and Methods

We analyze the recent compilation of model large ensembles of simulations from CMIP5-generation models compiled by the US climate variability and predictability (CLIVAR) Large Ensemble Working Group (Deser et al., 2020). This collection comprises output from seven models with 20–100 ensemble members each. We also analyze ensembles of simulations from twelve CMIP6 models that ran at least 10 historical simulations each. All of the models that we include in this study are fully coupled atmosphere, land, ocean and sea ice component models.

The simulations were forced with best estimates of the greenhouse gas, ozone, solar and aerosol forcing since 1850. The ensembles begin as early as 1850 and run approximately to present day (2005 for the CLIVAR models and 2014 for the CMIP6-generation models.) We note that for the EC-Earth3 model, only 23 ensemble members were run for the period 1850–1969, with the additional 50 members beginning in 1970. We also note that sea ice output was not available for the EC-Earth model, so only the temperature response is presented for that model. Details of each ensemble are summarized in Table 1. We also compare the global mean surface temperature evolution following volcanic eruptions with the GISTEMP (GISTEMP Team, 2020; Lenssen et al., 2019) and Berkeley Earth (Rohde et al., 2013) observational datasets.

We assess statistical significance of the zonal-mean temperature anomalies with a 2-tailed Student's t-test at the 95% confidence level, and assess field significance, correcting for the effect of multiple testing, using the false discovery rate (FDR) criterion of (Wilks, 2016), with FDR $\alpha_{FDR} = 0.1$. We then compute thresholds for significance by inverting the formula for the t-statistic to compute the anomaly needed to achieve significance given the critical p-value needed to satisfy the FDR criterion.

Table 1
Details of the Models Used.

Model	Members	Years	Reference
CanESM2	50	1950–2100	(Kirchmeier-Young et al., 2017)
CESM1-CAM5	40	1920–2100	(Kay et al., 2015)
EC-Earth	16	1860–2100	(Hazeleger et al., 2010)
CSIRO-Mk3-6-0	30	1850–2100	(Jeffrey et al., 2013)
GFDL-CM3	20	1920–2100	(Sun et al., 2018)
GFDL-ESM2M	30	1950–2100	(Rodgers et al., 2015)
MPI-ESM	100	1850–2100	(Maher et al., 2019)
ACCESS-ESM1-5	30	1850–2014	(Ziehn et al., 2020)
CanESM5	50	1850–2014	(Swart et al., 2019)
CESM2	11	1850–2014	(Danabasoglu et al., 2020)
CNRM-CM6-1	30 (21)	1850–2014	(Voldoire et al., 2019)
EC-Earth3	73	1850–2014	(Hazeleger et al., 2010)
GISS-E2-1-G	46	1850–2014	(Kelley et al., 2020)
GISS-E2-1-H	23	1850–2014	(Kelley et al., 2020)
IPSL-CM6A-LR	32	1850–2014	(Boucher et al., 2020)
MIROC6	50	1850–2014	(Tatebe et al., 2019)
MPI-ESM1-2-LR	10	1850–2014	(Mauritsen et al., 2019)
MPI-ESM1-2-HR	10	1850–2014	(Gutjahr et al., 2019)
UKESM1-0-LL	17	1850–2014	(Sellar et al., 2019)

The first seven are from the CLIVAR collection of large ensembles using CMIP5 radiative forcings, and the remainder are from the CMIP6 models that ran at least 10 historical simulations each. The number in parentheses denotes the number of ensemble members for which sea ice output is available, where that differs from the number for which surface temperature is available.

3. Results

In order to verify that the models analyzed produce the correct global response to historical volcanic eruptions, we examine the global mean surface temperature (GMST) response for each ensemble, and compare to two observational datasets. GMST decreases by about 0.2 K following both the Pinatubo eruption in 1991 and the Agung eruption in 1963 in both models and observations (see Figure 1). The CMIP6-generation models tend to better reproduce the observed cooling following the Pinatubo eruption, while most of the CLIVAR models tend to overestimate the cooling (although the difference is modest and based on a relatively small set of models). The temperature decrease following the El Chichon eruption in 1982 is generally larger in models than in observations, with no discernible cooling in the observations. Previous studies have shown that the small cooling response to the El Chichon eruption is due to the strong El Niño in the same year as the eruption offsetting the volcanically induced cooling (e.g., Lehner et al., 2016). Since the focus of our study is the Pinatubo eruption, when there was also an El Niño in the year of the eruption, we computed the temperature response that would have been observed if the El Niño did not occur. We assume that the influence of ENSO is averaged out in the model ensemble mean and removed the ENSO signal from both observational products by regressing out the second principal component of global SSTs (the first corresponds to the global warming pattern) for each product. With ENSO removed, the cooling following Pinatubo was about 0.025°C greater in both observational products, which is still well within the model spread.

Hereafter, we focus on the response to the Pinatubo eruption in June 1991, due to the large cooling response associated with it and the approximately symmetric forcing it produced, due to transport of stratospheric aerosols into both hemispheres. We show results for the El Chichon and Agung eruptions in the Supporting Information. Further, based on the observation that the largest cooling in response to the Pinatubo eruption occurs about one year after the eruption, we define the response as the difference beginning June

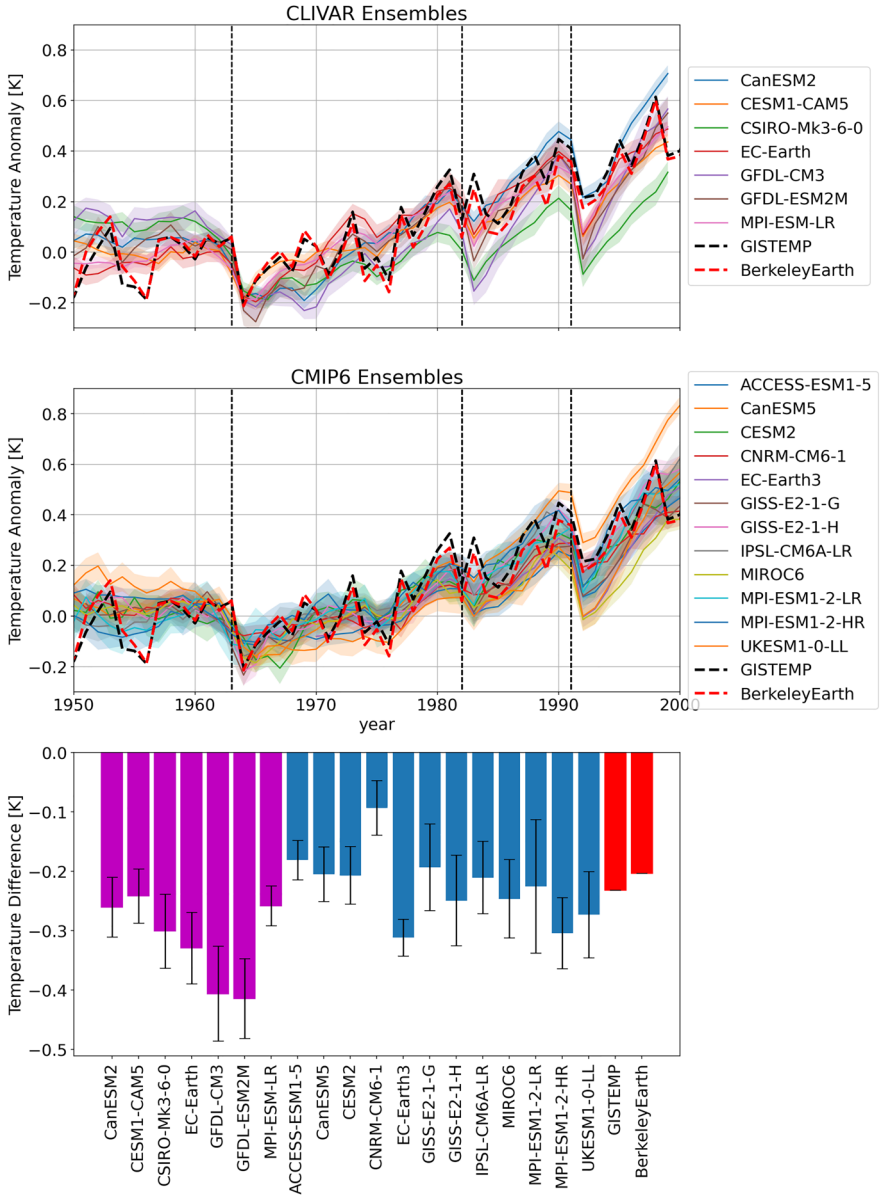

Figure 1. Annual GMST anomaly from 1951 to 1980 mean for (top) the CLIVAR large ensembles and (middle) the CMIP6 large ensembles. The black and red dashed lines on both denote the observed annual GMST anomaly from two different products. Shading denotes the 5–95% confidence interval about each model's ensemble mean. Vertical black dashed lines denote the year of the three major eruptions in the historical period (bottom) GMST difference of 1992 minus 1990 annual means for the ensemble mean of each model. Magenta bars denote CLIVAR models, blue bars denote CMIP6 models, and red bars denote observations. Errorbars denote the 95% confidence interval for the ensemble mean. In this figure, annual means are January-December mean of each year.

1992 relative to the year prior to the eruption beginning June 1990. Despite this short reference period, the large number of ensemble members in the models analyzed here allow us to greatly reduce the influence of internal variability.

We next examine the zonal-mean surface temperature response in the year following the Pinatubo eruption for each ensemble. In the ensemble mean of almost all models, there is significant cooling in the mid-latitudes between about 50°S and 50°N (Figure 2). For most of the CLIVAR models there is also significant cooling at the northern high-latitudes, whereas the cooling signal over the southern high latitudes is more equivocal. Most CMIP6-generation models have a northern high-latitude cooling, however the response is

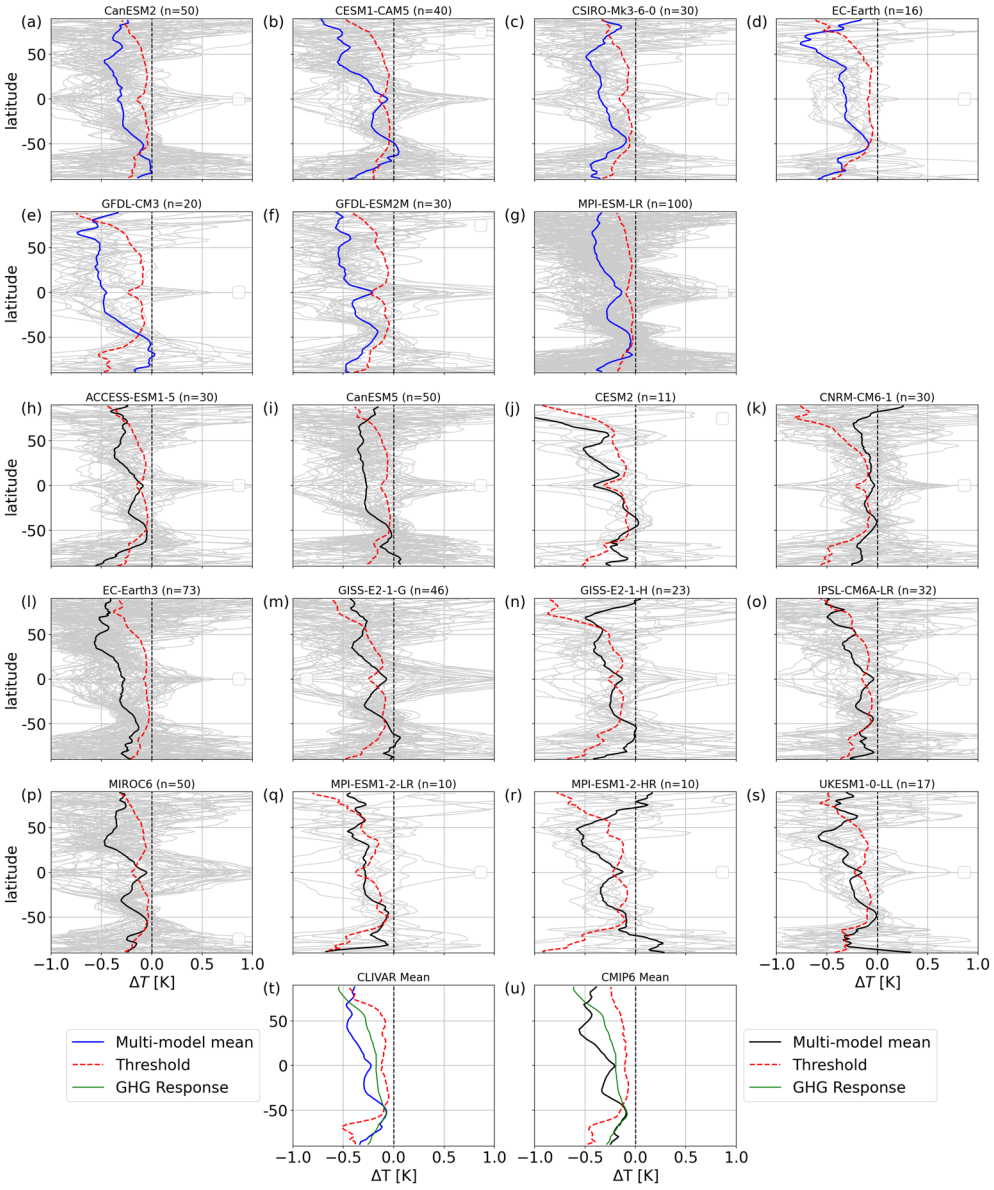

Figure 2. Zonal-mean surface temperature response for each of the CLIVAR (a–g) and CMIP6 (h–s) large ensembles (t) and (u) show the multi-model mean response for the CLIVAR and CMIP6 collections respectively. Each response is the difference between the mean of June 1992–May 1993 and the mean of June 1990–May 1991. Gray lines denote individual ensemble members and the heavy blue and black lines denote the ensemble means for the CLIVAR and CMIP6 ensembles, respectively. Red dashed lines denote the threshold for the anomaly to exceed the critical p-value as determined by the false discovery rate criterion of (Wilks, 2016) with $\alpha_{FDR} = 0.1$. Also shown in (t) and (u) is the multi-model mean fast response to greenhouse gas forcing, computed as the mean anomaly between the first 10 years of the abrupt-4xCO2 simulations and the corresponding pre-industrial control runs. The greenhouse gas response is scaled to have the same variance as the multi-model mean response to Pinatubo, and has the sign reversed. CLIVAR, climate variability and predictability; CMIP, Coupled Model Intercomparison Project Phase 6.

not always statistically significant, possibly due to the generally smaller ensemble sizes. There is substantial spread in the CMIP6 southern high-latitude response, with some models displaying cooling and others displaying only a weak temperature response. In general, the cooling in the multi-model mean of the CLIVAR models is about the same as that in the multi-model mean of the CMIP6-generation models (see Figures 2t and 2u). The spread of the temperature anomaly across ensemble members is greatest in the polar regions and the tropics, the former likely due to the variability associated with the spread in sea ice cover across

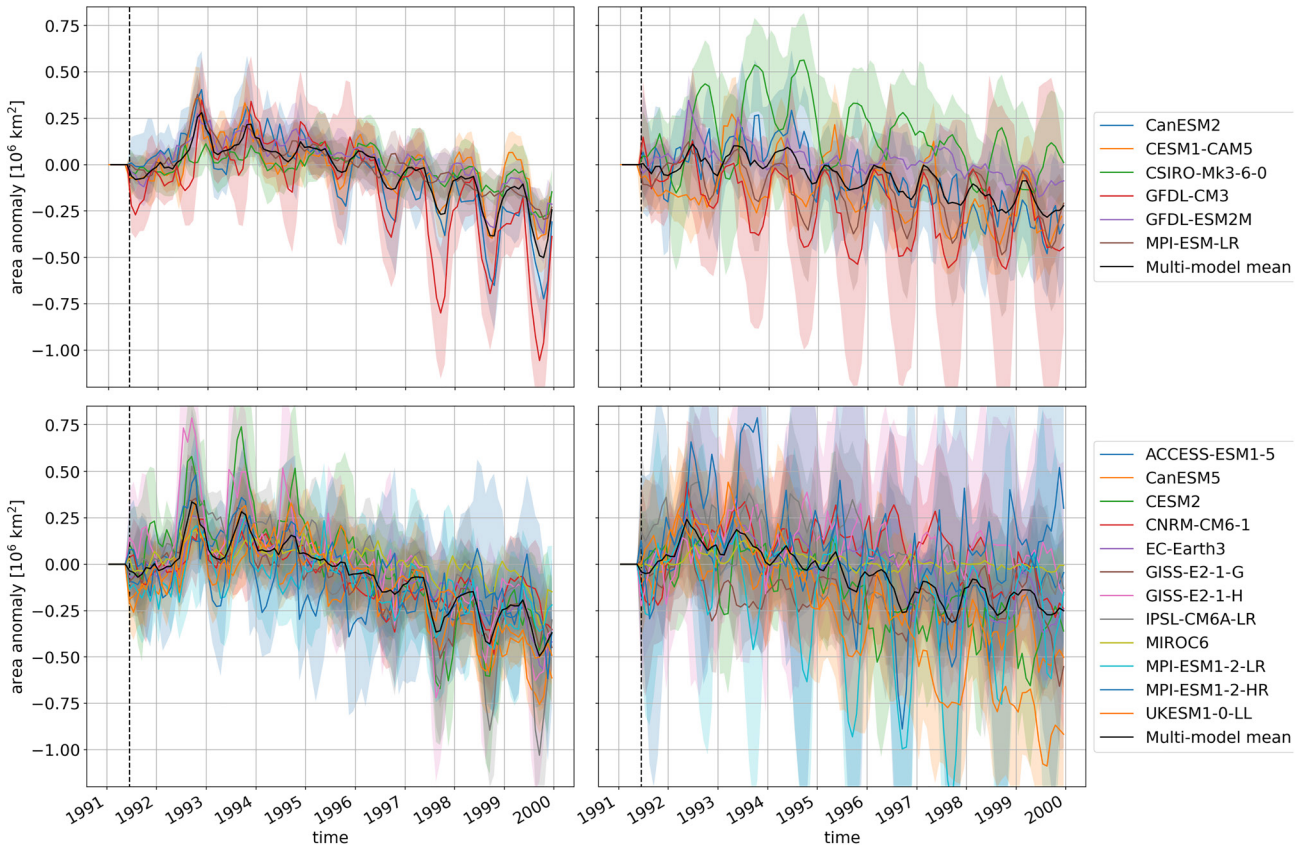

Figure 3. Monthly sea ice area response for the ensemble mean of each model from (top row) CLIVAR and (bottom row) CMIP6 for (left column) Arctic and (right column) Antarctic. The monthly response is defined as the mean of a month in given year minus the mean of that month from the reference year of June 1990–May 1991. Shading represents the 95% confidence interval for the ensemble mean, and the vertical dashed lines denote the time of the eruption. CLIVAR, climate variability and predictability; CMIP, Coupled Model Intercomparison Project Phase 6.

ensemble members. The peak in variability in the tropics is associated with the spread in the state of the El Niño Southern Oscillation (ENSO) across ensemble members (Supporting Information), and is not associated with the forcing due to the eruption. Further, the ensemble mean of a large ensemble should result in the phase of ENSO being averaged out.

For about 4 years following the eruptions, Arctic sea ice area is larger than the reference year (see Figure 3), with the peak increase each year in September, at the end of the Arctic sea ice melt season. The timing of the peak sea ice area increase is consistent with a combination of the seasonal nature of the shortwave forcing due to volcanic aerosols and the tendency for sea ice anomalies to accumulate over the melt season, since that is when positive feedbacks are active. The peak sea ice area response is delayed by about one year from the time of the eruption, owing to the time for aerosols to be transported to the Arctic via the Brewer-Dobson circulation. The response in the Antarctic sea ice area is less consistent, with the response differing in sign and seasonality across models. This hemispheric asymmetry in the sea ice area response is consistent with the results of Zanchettin et al. (2014).

Arctic sea ice volume increases in response to the Pinatubo eruption in both model generations (see Figure 4), peaking in October-November of 1992 in most models. The sea ice volume response is larger and persists much longer for the Community Earth System Model version 2 (CESM2) than for the other models, peaking in the winter of 1993–1994. It is unclear why CESM2 has such a strong sea ice volume response. The seasonality of the sea ice volume response is weaker than that of the sea ice area, consistent with the greater persistence of sea ice volume anomalies compared to sea ice area (Blanchard-Wrigglesworth et al., 2011). Most models have a local maximum response in September of 1992, after which the time-of-year of the peak response varies across models. As with the sea ice area response, there is little response of Antarctic sea ice

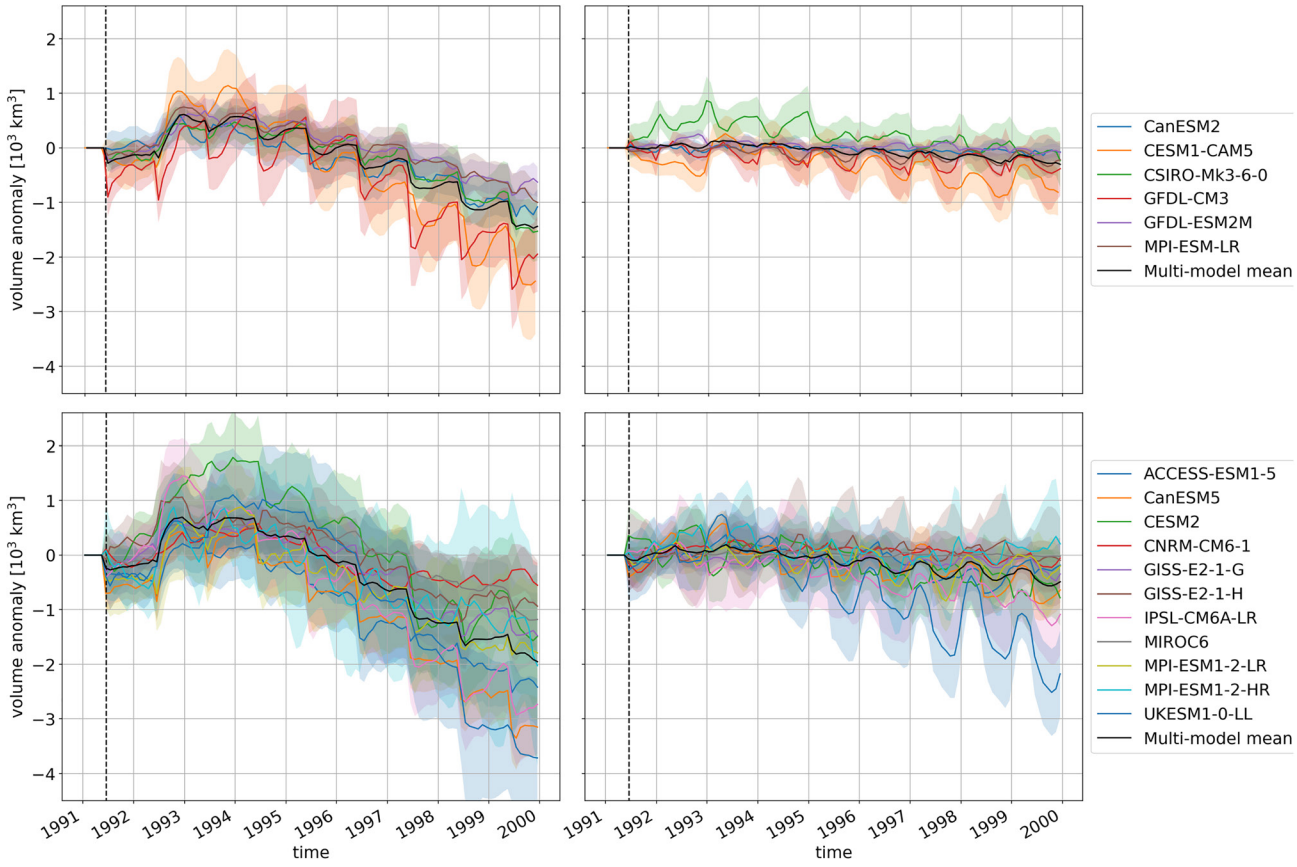

Figure 4. As in Figure 3 but for sea ice volume.

volume to the Pinatubo eruption. There is no discernible increase in sea ice volume following the eruption, and the decrease after about 1996 in some models can be attributed to greenhouse gases.

4. Discussion

The response of the climate system to volcanic aerosols can be obscured by internal climate variability (e.g., ENSO can be a factor for even the GMST response) and other climate forcings. We've alleviated these issues by analyzing model large ensembles that facilitate separation of the forced response from internal variability and by focusing on recent large volcanoes whose forcing overwhelms other climate forcings over short time periods. By inter-comparing results from a number of models we can infer the robust response to volcanoes.

We found that the hemispheric asymmetry in the zonal-mean surface temperature response under the approximately symmetric radiative forcing due to the Pinatubo eruption seen in Yang et al. (2019) is reproduced by almost all of the CLIVAR large ensembles and many of the CMIP6 ensembles. In the multi-model mean for both model collections, the cooling response is statistically significant over the entire Northern Hemisphere and low-latitude Southern Hemisphere. However, the response is not significant over the high-latitude Southern Hemisphere, due to the weaker response and large variability in that region. It is worth noting that, although the ensemble-mean response is significant over much of the globe in most of the models analyzed here, individual ensemble members do not necessarily have a cooling response at all of these latitudes. Particularly at high latitudes, many individual ensemble members warm following the Pinatubo eruption. This result suggests that we are not guaranteed to experience cooling after a Pinatubo-sized eruption at any given latitude, especially at high latitudes. This result is similar to that of Polvani et al. (2019), who found substantial wintertime warming in the Arctic following the Pinatubo eruption in individual model ensembles members, despite no significant response in the multi-model mean. To confirm

this result we examined the zonal-mean temperature response to the Pinatubo eruption as a function of month, and indeed found weak warming in the Arctic in the boreal winter following the eruption (e.g., Shindell et al., 2004), followed by cooling in the subsequent summer and fall (Supporting Information).

In the ensemble mean of almost all models, there is a local minimum in the response to the Pinatubo eruption in the Southern Ocean, indicating that the cooling response is damped in that region. The studies of Yang et al. (2019) and Zanchettin et al. (2014) found a similar response in their single-model ensembles with only volcanic forcing. Zanchettin et al. (2014) attributed this response to a smaller change in the atmospheric heat transport in the Southern Hemisphere and local feedback processes in the Southern Ocean and Antarctic regions. That we see a similar response across model large ensembles, with which we have been able to reduce the influence of internal variability and greenhouse gas forcing, indicates that the inter-hemispheric asymmetry in the temperature response is a robust feature of the climate system response to approximately hemispherically symmetric volcanic forcing.

The damped cooling response in the Southern Ocean is reminiscent of the damped warming in the region in the short-term response to greenhouse gas forcing (see Supplementary Information and Figures 2t and 2u). This damping in either case is notable despite differences in the physical nature of the forcing, with greenhouse gases primarily reducing outgoing longwave radiation and volcanic aerosols mostly reducing incoming shortwave radiation. The weak short-term response of the Southern Ocean in response to increased atmospheric greenhouse gas concentrations was explained in early studies as predominantly due to the deep vertical mixing in the Southern Ocean, resulting in a higher effective heat capacity and associated greater thermal inertia in that region (e.g., Manabe et al., 1991). More recent studies have instead attributed the delayed warming to the meridional overturning circulation of the Southern Ocean, via wind-driven upwelling of deep water and subsequent equatorward heat transport (e.g., Armour et al., 2016).

The GMST response in the CMIP6 models is in better agreement with the observations for the Pinatubo eruption than that in the CMIP5 generation models. The study of Gregory et al. (2016) also found that CMIP5 models tended to overestimate the cooling associated with a volcanic eruption. Unfortunately, we cannot differentiate attribution of this overestimate in CMIP5-generation models to the radiative forcing of volcanoes versus the model's sensitivity to volcanic aerosols because CMIP5 did not include sufficient experiments to separate these effects. We also note that, unlike in CMIP6, the volcanic forcing used in CMIP5-generation models was left to the discretion of the individual modeling centers, which adds further complication in determining the role of forcing changes. CMIP6 models have been shown to have higher overall effective climate sensitivity than those from the CMIP5 generation (e.g., Zelinka et al., 2020). Comparing each model's global mean surface temperature response to its effective climate sensitivity (Supporting Information), we found no relationship, indicating that this is not the reason for the differing response to Pinatubo between model generations.

The sea ice response to the Pinatubo eruption also exhibits marked asymmetry between the two hemispheres, with a much stronger response in the Arctic than in the Antarctic. This asymmetry is in agreement with the results of Zanchettin et al. (2014) in their single-model ensemble with only volcanic forcing, indicating that it is a robust feature of the climate system response to approximately symmetric volcanic forcing. The peak response in both Arctic sea ice area and volume occurs in September of the year following the eruption. This delayed response is due to the time taken for the aerosols to be transported to the polar regions, and that, due to the shortwave nature of the forcing, the effect accumulates over the summer months, when there is sunlight in the Arctic. The strong agreement across different models shown in our results suggests that we would expect to see an increase in Arctic sea ice area and volume for a few years following an eruption of the scale of Pinatubo, however such an increase is not guaranteed due to the large internal variability in this region.

Overall, our study confirms the results of previous studies with idealized forcing in individual model ensembles across a large collection of model ensembles and in the presence of other forcings. The use of these large ensembles of multiple models allows us to state with greater confidence that the asymmetric response of the climate system to the approximately symmetric forcing of a Pinatubo-sized eruption is a robust feature of the system, and is reminiscent of the well-known asymmetric fast response to greenhouse gas forcing, despite the very different physical nature of the forcing.

Data Availability Statement

The CMIP6 data are available at https://esgf-node.llnl.gov/projects/esgf-llnl. Data from the Multi-Model Large Ensemble Archive are available at https://www.cesm.ucar.edu/projects/community-projects/MMLEA. The Berkeley Earth temperature data are available at http://berkeleyearth.org/data/. The GISTEMP data are available at https://data.giss.nasa.gov/gistemp/.

Acknowledgments
Support for this project was provided by NOAA project number NA18OAR4310274. The authors acknowledge the CLIVAR Working Group on Large Ensembles for making the model output available. The authors acknowledge the World Climate Research Programme (WRCP), which, through its Working Group on Coupled Modeling, coordinated and promoted CMIP6. The authors thank the climate modeling groups for producing and making available their model output, the Earth System Grid Federation (ESGF) for archiving the data and providing access, and the multiple funding agencies who support CMIP6 and ESGF. The authors thank Dargan Frierson, Gabriel Vecchi, Wenchang Yang, and Emma McMahon for stimulating discussions.

References

Armour, K. C., Marshall, J., Scott, J. R., Donohoe, A., & Newsom, E. R. (2016). Southern Ocean warming delayed by circumpolar upwelling and equatorward transport. *Nature Geoscience*, *9*(7), 549–554. https://doi.org/10.1038/ngeo2731

Blanchard-Wrigglesworth, E., Armour, K. C., Bitz, C. M., & DeWeaver, E. (2011). Persistence and inherent predictability of Arctic Sea Ice in a GCM ensemble and observations. *Journal of Climate*, *24*(1), 231–250. https://doi.org/10.1175/2010JCLI3775.1

Boucher, O., Servonnat, J., Albright, A. L., Aumont, O., Balkanski, Y., Bastrikov, V., et al. (2020). Presentation and evaluation of the IPSL-CM6A-LR Climate Model. *Journal of Advances in Modeling Earth Systems*, *12*(7), e2019MS002010. https://doi.org/10.1029/2019MS002010

Danabasoglu, G., Lamarque, J. F., Bacmeister, J., Bailey, D. A., DuVivier, A. K., Edwards, J., et al. (2020). The Community Earth System Model Version 2 (CESM2). *Journal of Advances in Modeling Earth Systems*, *12*(2), e2019MS001916. https://doi.org/10.1029/2019MS001916

Deser, C., Lehner, F., Rodgers, K. B., Ault, T., Delworth, T. L., DiNezio, P. N., et al. (2020). Insights from Earth system model initial-condition large ensembles and future prospects. *Nature Climate Change*, *10*(4), 277–286. https://doi.org/10.1038/s41558-020-0731-2

Ding, Y., Carton, J. A., Chepurin, G. A., Stenchikov, G., Robock, A., Sentman, L. T., & Krasting, J. P. (2014). Ocean response to volcanic eruptions in Coupled Model Intercomparison Project 5 simulations. *Journal of Geophysical Research: Oceans*, *119*(9), 5622–5637. https://doi.org/10.1002/2013JC009780

Eyring, V., Bony, S., Meehl, G. A., Senior, C. A., Stevens, B., Stouffer, R. J., & Taylor, K. E. (2016). Overview of the Coupled Model Intercomparison Project Phase 6 (CMIP6) experimental design and organization. *Geoscientific Model Development*, *9*, 1937–1958. https://doi.org/10.5194/gmd-9-1937-2016

Gagné, M.-È., Kirchmeier-Young, M. C., Gillett, N. P., & Fyfe, J. C. (2017). Arctic sea ice response to the eruptions of Agung, El Chichón, and Pinatubo. *Journal of Geophysical Research - D: Atmospheres*, *122*(15), 8071–8078. https://doi.org/10.1002/2017JD027038

GISTEMP Team. (2020). *GISS Surface Temperature Analysis (GISTEMP) version 4*. NASA Goddard Institute for Space Studies. Retrieved 2020-08-28, from https://data.giss.nasa.gov/gistemp/

Gregory, J. M., Andrews, T., Good, P., Mauritsen, T., & Forster, P. M. (2016). Small global-mean cooling due to volcanic radiative forcing. *Climate Dynamics*, *47*(12), 3979–3991. https://doi.org/10.1007/s00382-016-3055-1

Gutjahr, O., Putrasahan, D., Lohmann, K., Jungclaus, J. H., von Storch, J.-S., Brüggemann, N., et al. (2019). Max Planck Institute Earth System Model (MPI-ESM1.2) for the High-Resolution Model Intercomparison Project (HighResMIP). *Geoscientific Model Development*, *12*(7), 3241–3281. https://doi.org/10.5194/gmd-12-3241-2019

Hazeleger, W., Severijns, C., Semmler, T., Ştefănescu, S., Yang, S., Wang, X., et al. (2010). EC-Earth. *Bulletin of the American Meteorological Society*, *91*(10), 1357–1364. https://doi.org/10.1175/2010BAMS2877.1

Jeffrey, S., Rotstayn, L., Collier, M., Dravitzki, S., Hamalainen, C., Moeseneder, C., et al. (2013). Australia's CMIP5 submission using the CSIRO-Mk3.6 model. *Australian Meteorological and Oceanographic Journal*, *63*(1), 1–14. https://doi.org/10.22499/2.6301.001

Kay, J. E., Deser, C., Phillips, A., Mai, A., Hannay, C., Strand, G., et al. (2015). The Community Earth System Model (CESM) Large Ensemble Project: A community resource for studying climate change in the presence of internal climate variability. *Bulletin of the American Meteorological Society*, *96*(8), 1333–1349. https://doi.org/10.1175/BAMS-D-13-00255.1

Kelley, M., Schmidt, G. A., Nazarenko, L. S., Bauer, S. E., Ruedy, R., Russell, G. L., et al. (2020). GISS-E2.1: Configurations and climatology. *Journal of Advances in Modeling Earth Systems*, *12*, e2019MS002025. https://doi.org/10.1029/2019MS002025

Kirchmeier-Young, M. C., Zwiers, F. W., & Gillett, N. P. (2017). Attribution of extreme events in Arctic Sea Ice Extent. *Journal of Climate*, *30*(2), 553–571. https://doi.org/10.1175/JCLI-D-16-0412.1

Lehner, F., Schurer, A. P., Hegerl, G. C., Deser, C., & Frölicher, T. L. (2016). The importance of ENSO phase during volcanic eruptions for detection and attribution. *Geophysical Research Letters*, *43*(6), 2851–2858. https://doi.org/10.1002/2016GL067935

Lenssen, N. J. L., Schmidt, G. A., Hansen, J. E., Menne, M. J., Persin, A., Ruedy, R., & Zyss, D. (2019). Improvements in the GISTEMP Uncertainty Model. *Journal of Geophysical Research: Atmospheres*, *124*(12), 6307–6326. https://doi.org/10.1029/2018JD029522

Maher, N., Milinski, S., Suarez-Gutierrez, L., Botzet, M., Dobrynin, M., Kornblueh, L., et al. (2019). The Max Planck Institute Grand Ensemble: Enabling the exploration of climate system variability. *Journal of Advances in Modeling Earth Systems*, *11*(7), 2050–2069. https://doi.org/10.1029/2019MS001639

Manabe, S., Stouffer, R. J., Spelman, M. J., & Bryan, K. (1991). Transient responses of a coupled ocean-atmosphere model to gradual changes of atmospheric CO2. Part I. Annual mean response. *Journal of Climate*, *4*(8), 785–818. https://doi.org/10.1175/1520-0442(1991)004⟨0785:TROACO⟩2.0.CO;210.1175/1520-0442(1991)004<0785:troaco>2.0.co;2

Mauritsen, T., Bader, J., Becker, T., Behrens, J., Bittner, M., Brokopf, R., et al. (2019). Developments in the MPI-M Earth System Model version 1.2 (MPI-ESM1.2) and its response to increasing CO2. *Journal of Advances in Modeling Earth Systems*, *11*(4), 998–1038. https://doi.org/10.1029/2018MS001400

Polvani, L. M., Banerjee, A., & Schmidt, A. (2019). Northern Hemisphere continental winter warming following the 1991 Mt. Pinatubo eruption: Reconciling models and observations. *Atmospheric Chemistry and Physics*, *19*(9), 6351–6366. https://doi.org/10.5194/acp-19-6351-2019

Robock, A. (2000). Volcanic eruptions and climate. *Reviews of Geophysics*, *38*(2), 191–219. https://doi.org/10.1029/1998RG000054

Rodgers, K. B., Lin, J., & Frölicher, T. L. (2015). Emergence of multiple ocean ecosystem drivers in a large ensemble suite with an Earth system model. *Biogeosciences*, *12*(11), 3301–3320. https://doi.org/10.5194/bg-12-3301-2015

Rohde, R., Muller, R. A., Jacobsen, R., Muller, E., Perlmutter, S., Rosenfeld, A., et al. (2013). A new estimate of the average earth surface land temperature spanning 1753 to 2011. *Geoinformatics and Geostatistics: An Overview*, *1*. https://doi.org/10.4172/2327-4581.1000101

Sellar, A. A., Jones, C. G., Mulcahy, J. P., Tang, Y., Yool, A., Wiltshire, A., et al. (2019). UKESM1: Description and evaluation of the U.K. Earth System Model. *Journal of Advances in Modeling Earth Systems*, *11*(12), 4513–4558. https://doi.org/10.1029/2019MS001739

Shindell, D. T., Schmidt, G. A., Mann, M. E., & Faluvegi, G. (2004). Dynamic winter climate response to large tropical volcanic eruptions since 1600. *Journal of Geophysical Research*, *109*(D5). https://doi.org/10.1029/2003JD004151

Stenchikov, G., Delworth, T. L., Ramaswamy, V., Stouffer, R. J., Wittenberg, A., & Zeng, F. (2009). Volcanic signals in oceans. *Journal of Geophysical Research*, *114*, D16104. https://doi.org/10.1029/2008JD011673

Sun, L., Alexander, M., & Deser, C. (2018). Evolution of the global coupled climate response to Arctic Sea ice loss during 1990-2090 and its contribution to climate change. *Journal of Climate*, *31*(19), 7823–7843. https://doi.org/10.1175/JCLI-D-18-0134.1

Swart, N. C., Cole, J. N. S., Kharin, V. V., Lazare, M., Scinocca, J. F., Gillett, N. P., et al. (2019). The Canadian Earth System Model version 5 (CanESM5.0.3). *Geoscientific Model Development*, *12*(11), 4823–4873. https://doi.org/10.5194/gmd-12-4823-2019

Tatebe, H., Ogura, T., Nitta, T., Komuro, Y., Ogochi, K., Takemura, T., et al. (2019). Description and basic evaluation of simulated mean state, internal variability, and climate sensitivity in MIROC6. *Geoscientific Model Development*, *12*(7), 2727–2765. https://doi.org/10.5194/gmd-12-2727-2019

Toohey, M., Krüger, K., Schmidt, H., Timmreck, C., Sigl, M., Stoffel, M., & Wilson, R. (2019). Disproportionately strong climate forcing from extratropical explosive volcanic eruptions. *Nature Geoscience*, *12*(2), 100–107. https://doi.org/10.1038/s41561-018-0286-2

Voldoire, A., Saint-Martin, D., Sénési, S., Decharme, B., Alias, A., Chevallier, M., et al. (2019). Evaluation of CMIP6 DECK experiments with CNRM-CM6-1. *Journal of Advances in Modeling Earth Systems*, *11*(7), 2177–2213. https://doi.org/10.1029/2019MS001683

Wilks, D. S. (2016). "The stippling shows statistically significant grid points": How research results are routinely overstated and overinterpreted, and what to do about it. *Bulletin of the American Meteorological Society*, *97*(12), 2263–2273. https://doi.org/10.1175/BAMS-D-15-00267.1

Yang, W., Vecchi, G. A., Fueglistaler, S., Horowitz, L. W., Luet, D. J., Muñoz, Á. G., et al. (2019). Climate impacts from large volcanic eruptions in a high-resolution climate model: The importance of forcing structure. *Geophysical Research Letters*, *46*(13), 7690–7699. https://doi.org/10.1029/2019GL082367

Zanchettin, D., Bothe, O., Timmreck, C., Bader, J., Beitsch, A., Graf, H.-F., et al. (2014). Inter-hemispheric asymmetry in the sea-ice response to volcanic forcing simulated by MPI-ESM (COSMOS-Mill). *Earth System Dynamics*, *5*(1), 223–242. https://doi.org/10.5194/esd-5-223-2014

Zelinka, M. D., Myers, T. A., McCoy, D. T., Po-Chedley, S., Caldwell, P. M., Ceppi, P., et al. (2020). Causes of higher climate sensitivity in CMIP6 models. *Geophysical Research Letters*, *47*(1). https://doi.org/10.1029/2019GL085782

Ziehn, T., Chamberlain, M. A., Law, R. M., Lenton, A., Bodman, R. W., Dix, M., et al. (2020). The Australian Earth System Model: ACCESS-ESM1.5. *Jshess*, *70*, 193–214. https://doi.org/10.1071/ES19035